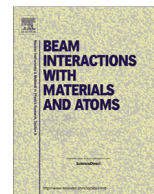




Contents lists available at ScienceDirect

Nuclear Instruments and Methods in Physics Research B

journal homepage: www.elsevier.com/locate/nimb

K, L, and M shell datasets for PIXE spectrum fitting and analysis



David D. Cohen*, Jagoda Crawford, Rainer Siegele

Australian Nuclear Science and Technology Organisation, Locked Bag 2001, Kirrawee, DC NSW 2232, Australia

ARTICLE INFO

Article history:

Received 19 February 2015

Received in revised form 16 July 2015

Accepted 6 August 2015

Available online 19 August 2015

Keywords:

PIXE

Fluorescence yields

Coster–Kronig transitions

Emission rates

Databases

ABSTRACT

Routine PIXE analysis programs, like GUPIX, GEOPIXE and PIXAN generally perform at least two key functions firstly, the fitting of K, L and M characteristic lines X-ray lines to a background, including unfolding of overlapping lines and secondly, the use of a fitted primary $K\alpha$, $L\alpha$ or $M\alpha$ line area to determine the elemental concentration in a given matrix. To achieve these two results to better than 3–5% the data sets for fluorescence yields, emission rates, Coster–Kronig transitions and ionisation cross sections should be determined to better than 3%.

There are many different theoretical and experimental K, L and M datasets for these parameters. How they are applied and used in analysis programs can vary the results obtained for both fitting and concentration determinations. Here we discuss several commonly used datasets for fluorescence yields, emission rates, Coster–Kronig transitions and ionisation cross sections for K, L and M subshells and suggests an optimum set to obtain consistent results for PIXE analyses across a range of elements with atomic numbers from $5 \leq Z \leq 100$.

© 2015 Elsevier B.V. All rights reserved.

1. Introduction

Particle induced X-ray emission (PIXE) has been around since the mid 1970's. It is now a mature technique used in over fifty PIXE laboratories worldwide. Many of these laboratories are using or have developed their own analysis software to both fit characteristic K, L and M shell X-ray lines and to determine elemental concentrations within a given substrate or matrix for a broad range of elements from carbon to uranium. GUPIX [1], GEOPIXE [2,3] and PIXAN [4,5] are three of many such codes that have been in common use for several decades. To be successful these codes require a broad range of datasets spanning much of the periodic table. With modern high speed computers it is now possible to quickly and efficiently calculate ionisation cross sections for inner shell vacancy production by most heavy ions. These inner shell ionisation cross sections then require well determined fluorescence yields, Coster–Kronig transition rates and single line emission rate datasets which are used to calculate line intensities and element concentrations. Well established PIXE codes should be capable of predicting line intensities and elemental concentrations to 3–5% for the K shell, provided they have these datasets to the same order of uncertainty [6]. However, such low levels of uncertainty for the L and M shell are problematic.

Here we discuss some of the commonly used datasets for fluorescence yields, emission rates, Coster–Kronig transitions and

ionisation cross sections for K, L and M subshells covering a broad range of target atomic number (Z) and quantitatively show the differences between these datasets. We also suggest our preferred optimum set to obtain reliable, self-consistent results for PIXE analyses across a range of atomic numbers from $5 \leq Z \leq 100$. We will not discuss here the effects of the choice of the X-ray mass attenuation coefficient datasets, on X-ray absorption, used in thick target analyses as this has been covered in a previous publication by Siegele et al. [7]. They recommended that the recent datasets of Chandler [8 and online] were preferred for PIXE analysis. We will also not consider here other input parameters, like X-ray energies, detector efficiencies and experimental geometries, which can also impact on the final analysis results. Most X-ray energies of interest to PIXE users (1–40 keV) are generally well determined compared to the uncertainties associated with the parameters considered here. The detector efficiencies and geometries are for the most situations specific to a given laboratory. Here we have chosen to focus on parameters that could be considered more generic and common to all users of analysis codes like GUPIX, GEOPIXE and PIXAN.

2. The PIXE datasets

The current literature contains an enormous quantity of both theoretical and experimental data required to convert inner shell vacancies generated by MeV light ions such as protons and helium ions to X-ray yields. It is not our intention to do a full review of these data here but to select a few of the most commonly used datasets relevant to thin target PIXE analysis which cover the

* Corresponding author. Tel.: +61 2 9717 3042.

E-mail address: dcz@ansto.gov.au (D.D. Cohen).

broadest possible range of elements across the periodic table and X-ray energies from 1 keV to 40 keV and to quantitatively investigate the variability between these different datasets.

Firstly, let us define a few common K, L and M shell equations to appropriately connect these individual data sets to the final PIXE X-ray yield results. For thin targets, the K, L and M shell X-ray yield in a peak p is a function of the X-ray production cross section $\sigma_{K,L,M}^X$ for that peak.

2.1. For the K shell

$$\sigma_{K_p}^X = \sigma_K^I \omega_K \frac{\Gamma_{K_p}}{\Gamma_K} \quad (1)$$

where, σ_K^I is the K shell ionisation cross section, ω_K is the K shell fluorescence yield and Γ_i is the emission rate for the peak $i = K_p$ and the $i = K$, the total K shell respectively.

2.2. For the L shell, with three subshells, L_1 , L_2 and L_3

Similar equations for the L_1 , L_2 and L_3 subshells for an L shell peak L_p are,

$${}^1\sigma_{L_p}^X = \sigma_1^I \omega_1 \frac{\Gamma_{L_p}}{\Gamma_{L_1}} \quad (2a)$$

$${}^2\sigma_{L_p}^X = (\sigma_1^I f_{12} + \sigma_2^I) \omega_2 \frac{\Gamma_{L_p}}{\Gamma_{L_2}} \quad (2b)$$

$${}^3\sigma_{L_p}^X = (\sigma_1^I (f_{12} f_{23} + f_{13} + f'_{13}) + \sigma_2^I f_{23} + \sigma_3^I) \omega_3 \frac{\Gamma_{L_p}}{\Gamma_{L_3}} \quad (2c)$$

where f_{ij} are the Coster Kronig transition probabilities for a vacancy moving from the i th subshell to the j th subshell within the L shell.

The total L shell X-ray production cross section is related to the total ionisation cross section by the average L shell fluorescence yield $\bar{\omega}_L$, where,

$$\sigma_{L_{tot}}^X = \bar{\omega}_L \sigma_{L_{tot}}^I \quad (2d)$$

where L_{tot} = sum of the three subshells L_1 , L_2 and L_3

2.3. For the M shell, with five subshells M_1 to M_5

Similar equations can be defined for the five M subshells as for the three L subshells, namely,

$${}^1\sigma_{M_p}^X = \sigma_1^I \omega_1 \frac{\Gamma_{M_p}}{\Gamma_{M_1}} \quad (3a)$$

$${}^2\sigma_{M_p}^X = (\sigma_1^I f_{12} + \sigma_2^I) \omega_2 \frac{\Gamma_{M_p}}{\Gamma_{M_2}} \quad (3b)$$

$${}^3\sigma_{M_p}^X = (\sigma_1^I (f_{12} f_{23} + f_{13}) + \sigma_2^I f_{23} + \sigma_3^I) \omega_3 \frac{\Gamma_{M_p}}{\Gamma_{M_3}} \quad (3c)$$

$${}^4\sigma_{M_p}^X = (\sigma_1^I (f_{14} + f_{12} f_{24} + f_{13} f_{34} + f_{12} f_{23} f_{34}) + \sigma_2^I (f_{24} + f_{23} f_{34}) + \sigma_3^I f_{34} + \sigma_4^I) \omega_4 \frac{\Gamma_{M_p}}{\Gamma_{M_4}} \quad (3d)$$

$${}^5\sigma_{M_p}^X = (\sigma_1^I (f_{15} + f_{12} f_{25} + f_{13} f_{35} + f_{14} f_{45} + f_{12} f_{23} f_{35}) + f_{12} f_{24} f_{45} + f_{12} f_{23} f_{34} f_{45}) + \sigma_2^I (f_{25} + f_{24} f_{45} + f_{23} f_{34} f_{45}) + \sigma_3^I (f_{35} + f_{34} f_{45}) + \sigma_4^I f_{45} + \sigma_5^I) \omega_5 \frac{\Gamma_{M_p}}{\Gamma_{M_5}} \quad (3e)$$

As with the L shell, the total M shell X-ray production cross section is related to the total M shell ionisation cross section by the average M shell fluorescence yield $\bar{\omega}_M$, where,

$$\sigma_{M_{tot}}^X = \bar{\omega}_M \sigma_{M_{tot}}^I \quad (3f)$$

and again M_{tot} is the sum of the five M subshells.

So if we are to predict the K, L and M shell X-ray line intensities for thin targets we need to have datasets for ionisation cross sections σ_{KLM}^I , for the fluorescence yields ω_{KLM} , for the line emission rates Γ_{KLM} and for the Coster–Kronig transitions f_{ij} . Clearly as we go from K to L to M subshells the situation becomes much more complex and much more difficult to measure experimentally or predict theoretically.

Table 1 shows the datasets we have selected for this study for the K, L and M shells and the range of ion energies and atomic number Z together with the references from which they were obtained. It is not exhaustive but does represent a broad cross section of datasets in common use by the PIXE community.

We have used the theoretical ionisation cross sections of the ECPSSR and ECUSAR calculations of Brandt and Lapicki [9] as these have general acceptance at the 5% level or better for MeV light ions (protons, deuterons and helium ions) on most targets with $6 \leq Z \leq 100$ for the K shell and a more restricted range for the L and M shells. Also we do not use the Scofield [30] relativistic Hartree Slater (RHS) compilations for K and L X-ray emission rates here but prefer the Scofield 1974 [16] relativistic Hartree Fock (HF) formulations for these emission rates as they are systematically larger and closer to the experimental measurements.

3. Results and discussion

3.1. Ionisation cross sections

The theoretical ECPSSR and ECUSAR ionisation cross sections of Brandt and Lapicki [9,18] have been widely used for many years and are generally accepted ionisation cross sections by the PIXE community. These cross sections are based on a series of corrections to the plane wave born approximation (PWBA) for inner shell vacancy production by light ions on heavy targets and include corrections for, energy loss (E) and Coulomb deflection (C) of the bombarding ion, the perturbed stationary states (PSS) of the target atom as the ion passes by and the relativistic nature of the inner shell electrons (R) particularly for the heavier target atoms. Furthermore, being a theoretical calculation these cross sections can be obtained for most light ions (protons, deuterons and alphas) on any target element in the periodic table from carbon to uranium and beyond. Also experiments performed over many decades show that for these light ions with energies well above 1 MeV/amu the ECPSSR and ECUSAR cross sections predict the average experimental data to better than a few percent for the K shell [31], 5–15% for the L shell and 10–50% for the M subshells [32].

Cohen and Harrigan [10,33,34] have tabulated the ECPSSR ionisation cross section for protons, deuterons and alphas for atomic numbers $6 \leq Z \leq 100$ for both K and L subshell ionisation as well as the L shell X-ray line intensities using the ECPSSR cross sections.

3.2. Inner shell fluorescence yields

The X-ray production cross sections are linked to the ionisation cross sections by the fluorescence yields, as shown in Eqs. (1)–(3) above. They are essentially the probability that an inner shell vacancy is filled by an outer electron and the emission of an X-ray usually in the keV energy range. We should state upfront that generally these fluorescence yields are for single hole vacancies only and do not include multiple vacancy which are clearly

Download English Version:

<https://daneshyari.com/en/article/1680158>

Download Persian Version:

<https://daneshyari.com/article/1680158>

[Daneshyari.com](https://daneshyari.com)